ARTICLE

Graphite Oxide Flame-Retardant Polymer Nanocomposites

Amanda L. Higginbotham,[†] Jay R. Lomeda,[†] Alexander B. Morgan,*[,‡] and James M. Tour*[,†]

Department of Chemistry, Rice University, 6100 Main Street, MS 222, Houston, Texas 77005, and Multiscale Composites and Polymers Division, University of Dayton Research Institute, 300 College Park, Dayton, Ohio 45469-0160

ABSTRACT Graphite oxide (GO) polymer nanocomposites were developed at 1, 5, and 10 wt % GO with polycarbonate (PC), acrylonitrile butadiene styrene, and high-impact polystyrene for the purpose of evaluating the flammability reduction and material properties of the resulting systems. The overall morphology and dispersion of GO within the polymer nanocomposites were studied by scanning electron microscopy and optical microscopy; GO was found to be well-dispersed throughout the matrix without the formation of large aggregates. Mechanical testing was performed using dynamic mechanical analysis to measure the storage modulus, which increased for all polymer systems with increased GO loading. Microscale oxygen consumption calorimetry revealed that the addition of GO reduced the total heat release and peak heat release rates in all systems, and GO−PC composites demonstrated very fast self-extinguishing times in vertical open flame tests, which are important to some regulatory fire safety applications.

KEYWORDS: graphite oxide • flame retardant • nanocomposites

INTRODUCTION

Although the prevention and control of fires is an important issue that has been addressed by many researchers, the problem is still prevalent and improvements are needed. It is estimated that each year death tolls related to fires exceed 4000 in the United States and 5000 in Europe, with costs totaling ~1% of the gross domestic product (1). The cause of fires can range between a wide combination of factors including the flammability of the generated volatiles, amount of heat released on burning, rate of heat release, ignitability of the material, etc.; therefore, it is critical to develop flame-retardant materials that are able to decrease both fire risks and hazards (1).

Polymers are the class of materials often targeted for flammability reduction in product fabrication because of their desirable mechanical, thermal, and electrical properties. Some inherently flame-retardant polymers such as poly(vinyl chloride) or fluoropolymers may be replaced by a more flammable polymer (such as a nonhalogenated polyolefin) because of cost constraints, recycle requirements, or regulations regarding the elimination of certain compounds (such as halogen or heavy metals) in waste electronic equipment, such as in the WEEE and RoHS protocols (2, 3). Alternative methods for improving the flammability of polymers without halogenated flame retardants involve the incorporation of additives such as alumina trihydrate and magnesium hydroxide. However, these additives must be used in very large quantities (>60 wt % for mineral fillers) for flame-retarding benefits to be realized, and this often has deleterious effects on the host polymer's mechanical and electrical properties (1). Phosphorus-based flame-retardant additives are another alternative, but these materials have their limitations as well including cost and plasticizing effects (depending upon the structure) on the polymer mechanical properties (4).

The formation of polymer nanocomposites has become a recent solution to improving the flammability of polymers via an additive approach. A nanocomposite in this context can be defined as a two-phase material whose filler is dispersed throughout the polymer on a nanometer scale. A significant advantage of nanoadditives is that they can be used in a much smaller amount (2−10 wt %) with markedly observed improvement in properties including enhanced mechanical properties, solvent resistance, and conductivity (5, 6). Lower filler requirements result in materials that are less expensive and easier to process. Carbon nanoadditives, including graphite and carbon nanotubes, have been extensively explored because of their ability to increase both the mechanical strength and electronic conductivity of the native polymer (7−9). In addition, carbon nanoadditives have begun to be explored for enhancement of the flame-retardant properties of various polymer systems. For example, expandable graphite has been used as an intumescent flame retardant in polyisocyanurate−polyurethane foams (10) and high-density rigid polyurethane foams (11) with an overall improvement of the fire behavior and no worsening of the mechanical properties. The incorporation of single-walled and multi-walled carbon nanotubes into polymers has demonstrated a decrease in the heat release rate, a slower combustion process, delayed time to ignition, and even an enhancement in the mechanical properties such as Young's modulus and the storage modulus (12−16).

One other carbon nanoadditive of interest is graphite oxide (GO). GO is the product obtained when bulk graphite

* To whom correspondence should be addressed. E-mail: Alexander.Morgan@udri.udayton.edu (A.B.M.), tour@rice.edu (J.M.T.).
Received for review June 18, 2009 and accepted August 31, 2009
[†] Rice University.
[‡] University of Dayton Research Institute.
DOI: 10.1021/am900419m

Published on Web 09/22/2009

is exposed to strong oxidizers such as sulfuric acid, nitric acid, potassium chlorate, or potassium permanganate. These introduce oxygen-containing functional groups, including hydroxyl and epoxy groups (17); the process is often employed to exfoliate or expand the graphene layers and to impart water solubility. The oxidation prevents graphene stacking and affords easy dispersion in both aqueous and polar organic media. The enhanced processability of GO allows it to be incorporated into polymer matrices, and the scalability and low cost of this process make it attractive for industrial applications (18). Chemical or thermal reduction can then be employed for partial recovery of the graphite structure; it has been shown that heating to only 200 °C will begin decomposition of the oxygen-containing functional groups to form thermally converted graphene (19). The flammability of GO has been studied in styrene–butyl acrylate and melamine–poly(metaphosphate) copolymers as well as poly(acrylic ester); the addition of GO was found to reduce the peak heat release rate by as much as 45% with only 1 wt % GO content (20–22). In addition, polystyrene systems containing modified GO experienced a 42% reduction in the peak heat release rate, with the additive not severely impacting the mechanical properties of the original polymer (23). Though these results are promising, the use of GO as a nanofiller for reducing the flammability of widely used commodity polymers is still lacking. Here we report the effect of GO addition into polycarbonate (PC), acrylonitrile–butadiene–styrene (ABS), and high-impact polystyrene (HIPS) on the mechanical strength and flammability of the resulting nanocomposites.

EXPERIMENTAL SECTION

Synthesis of Graphite Oxide (GO). GO was synthesized from expanded graphite obtained from SupraCarbonics, LLC, using the Staudenmaier procedure (19, 24). Briefly, 5 g (416.7 mmol of C) of expanded graphite was added in five portions to a stirred mixture of concentrated H_2SO_4 (87.5 mL) and fuming HNO_3 (45 mL) during cooling in an ice–water bath. To the mixture was added $KClO_3$ (55 g, 0.45 mol) in 11 separate and equal portions, each added to the reaction mixture 15 min apart while ensuring sufficient venting using nitrogen gas to reduce the risk of explosion upon generation of chlorine dioxide gas. (**Caution!** *Protective equipment including face shield, acid-resistant gloves, and blast shield must be used at all times.*) The resulting slurry was stirred at room temperature for 96 h. The green slurry was poured into 4 L of ice water, and the mixture was filtered and subsequently washed with 5 L of 5% HCl. The filter cake was then rinsed thoroughly with water until the filtrate was neutral. The filter cake was then dispersed in methanol (300 mL, vigorous stirring) and precipitated with diethyl ether (350 mL) followed by a final, thorough rinse with diethyl ether to yield 4.1 g of a fine brown powder of GO.

Formation of GO Nanocomposites. The resin (10 g; PC, Dow Calibre 301-10; ABS, Dow Magnum 9010; or HIPS, Dow Styron 478) was soaked overnight in 200 mL of tetrahydrofuran (THF) (PC and HIPS) or chloroform ($CHCl_3$) (ABS) to expand the polymer and begin dissolution. Complete dissolution was achieved the next day by vigorous stirring with a metal spatula and/or application of heat to the system. In a separate container, GO (in the amount to reach the overall desired weight percentage in the system) was high-shear-mixed (IKA T-25 digital ULTRA-TURRAX disperser with 18 G dispersing element, 7000 rpm) for 30 min in ~100 mL of the same solvent as that used to dissolve the polymer. The GO suspension was then poured into the dissolved polymer solution and high-shear-mixed for 30 min. To precipitate the GO polymer composite, the mixture was *slowly* added to a 5× volume of methanol (for THF solutions) or diethyl ether (for the $CHCl_3$ solution) (~1500 mL) with vigorous stirring. The GO composite was isolated by filtering over a poly(tetrafluoroethylene) membrane (5 μm pore size), washed with methanol or diethyl ether, and allowed to dry completely. Sample bars suitable for open flame testing and dynamic mechanical analysis (DMA) were prepared via melt extrusion (CSI-183MMX Mini Max extruding system). The GO composite was heated until molten and then extruded into a heated stainless steel mold (80 °C, width 1.3 cm, length 7.6 cm, thickness 0.3 cm) at a processing temperature of 270 °C (PC), 240 °C (ABS), or 250 °C (HIPS).

Vertical Open Flame Testing. The method used was a modified version of ASTM D3801. Rectangular bars measuring 1.3 cm wide, 7.6 cm long, and 0.3 cm thick were used, and all tests were done in an Atlas Electric HVUL-94 flame test station. The methane tank pressure regulator was set to 23 psi; the pressure regulator on the HVUL-94 test station was set to 5 psi. The Bunsen burner flame height was 55 mm, and the height from the top of the Bunsen burner to the bottom of the test bar was 40 mm; therefore, the sample overlapped with the flame by ~15 mm. All test bars underwent one trial, where the bar was exposed to a 10 s ignition followed by flame removal and the time to self-extinguish was recorded.

Microcombustion Calorimetry (MCC) Testing. MCC tests (MCC-1, Govmark) were run under nitrogen at a heating rate of 1 °C/s from 250 to 750 °C using method A of ASTM D7309 (pyrolysis under nitrogen). Each sample was run in triplicate to evaluate the reproducibility of the flammability measurements.

Thermogravimetric Analysis (TGA). TGA (Q50, TA Instruments) was conducted from room temperature to 950 °C at 10 °C/min under argon.

DMA. DMA (Q800, TA Instruments) was performed with a dual-cantilever clamp on sample bars measuring 1.3 cm wide, 7.6 cm long, and 0.3 cm thick. A temperature ramp experiment (3 °C/min) was conducted under air from room temperature to 150 °C (ABS and HIPS systems) or 180 °C (PC systems) at a constant frequency of 1 Hz.

Scanning Electron Microscopy (SEM). SEM images were obtained at 5.0 kV on freeze-fractured cross sections of the respective GO/polymer composite sample bar. Before imaging, the samples were coated with a 20 nm layer of gold to minimize charging.

Optical Microscopy. The samples were imaged using a polarizing optical microscope (Zeiss Axioplan-2) by first melting a small portion of the polymer composite by heating in an oven and then pressing a thin layer onto a glass microscope slide.

RESULTS AND DISCUSSION

The nanocomposites of GO were solvent-blended with PC, ABS, and HIPS at varying weight percentages; the resins were chosen because of their use in many engineering plastics applications. PC is somewhat inherently flame-retardant because of its ability to form polyaromatic char and release CO_2 upon ignition, while ABS and HIPS are considerably more flammable (25). Therefore, the wide range of properties between the resins will allow for a broad evaluation of the ability of GO to reduce the flammability of commodity polymers. In order to determine the quality of the composites, the overall morphology and dispersion of GO were studied by SEM and optical microscopy. In addition, the mechanical properties of the composites were evaluated using DMA; the storage modulus and glass transi-

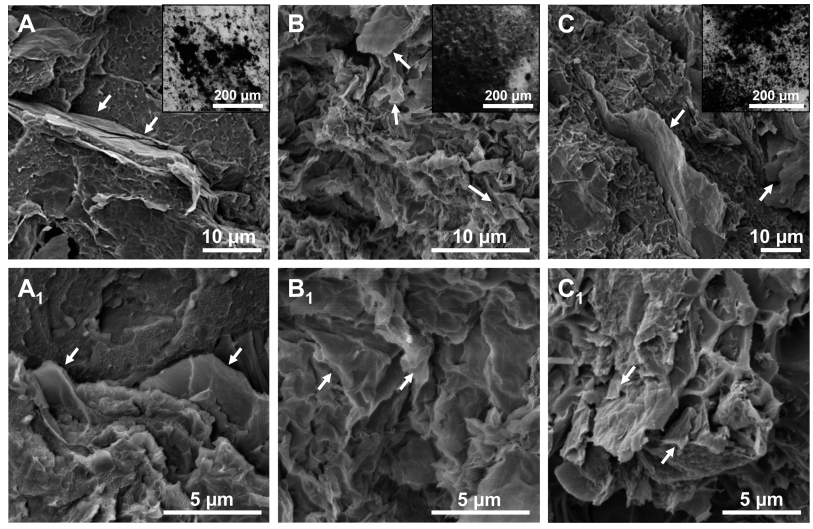

FIGURE 1. SEM and optical microscopy images (inset) of 10 wt % GO loaded in HIPS (A), ABS (B), and PC (C) composites. The bottom row of images shows zoomed-in regions of the sample directly above. The white arrows highlight some of the areas that contain GO flakes. For all samples, it is apparent that the GO flakes do not form large agglomerates and are dispersed throughout all sample regions imaged.

tion temperature were measured. To evaluate the thermal properties and flammability of the materials, MCC, TGA, and vertical open flame testing were performed.

Sample Imaging. SEM images (Figure 1) taken of the composites at their fracture surface reveal that overall the GO flakes do not agglomerate into dense regions. GO flakes were present throughout, and no large, noticeable features were found, suggesting good dispersion. The images shown in Figure 1 are for HIPS, ABS, and PC composites containing 10 wt % GO. Flakes of GO, several micrometers in size, were found protruding from the polymer matrix and are indicated by the white arrows. Optical microscopy supports the SEM data but points to adequate dispersions at the microscale (Figure 1, inset) due to the observation of dark regions, presumed to be GO, present in all parts of the sample. Although the concentration of the dark regions is not always evenly distributed, this may be attributed to the manner in which the optical samples were prepared; the polymer samples were heated to the point of softening and flattened on a glass microscope slide before imaging so that the light passing through the sample was maximized. Many regions were completely filled with GO and thus unable to be optically imaged.

Mechanical Properties. To study the effects of GO addition on the mechanical properties of the polymers, the storage modulus of the composites was measured using DMA. A dual-cantilever clamp was used on sample bars measuring 1.3 cm wide, 7.6 cm long, and 0.3 cm thick; the samples were heated in air at 3 °C/min to 150 °C (ABS and HIPS) or 180 °C (PC). It was observed with all three polymers that the storage modulus increased with increasing GO content over the entire temperature range (Figure 2). Although the increase in strength is not proportional to the amount of GO added, it does not immediately appear that incorporation of the nanofiller has deteriorated the mechanical properties of the polymer. Further analysis of the impact, tensile, and flexural strength is necessary to determine the overall effect the GO addition has on the mechanical strength of the native polymer. The most distinct increase in the storage modulus with increasing GO content was observed for HIPS, while PC showed only a small increase, with 5 and 10 wt % GO samples having almost identical storage moduli across the entire temperature range. The glass transition temperature (T_g) was extrapolated from the storage modulus data and found to not vary significantly with increasing GO content. In general, T_g increased slightly with increasing GO, implying that GO addition increases the stiffness of the composites. T_g for each sample is given in the inset of Figure 2.

Thermal and Flammability Properties. Several techniques were employed to assess the thermal and flammability properties of the GO−polymer composites including MCC, TGA, and vertical open flame testing. The microcombustion calorimeter is a small-scale instrument that measures the heat release of a material by oxygen consumption calorimetry and has been recently employed as a small-scale alternative to the cone calorimeter when the sample supply is limited (26). The heat of combustion of pyrolysis products is measured, and the heat release can be used to predict the flammability of the material (27). Using this technique, the samples are exposed to a fast heating rate to mimic fire-type conditions. The experiment consists of first pyrolyzing the sample under an inert atmosphere (nitrogen in this case) at a heating rate of 1 °C/s from 250 to 750 °C (using method A of ASTM D7309) and then pushing the pyrolysis products into a 900 °C combustion furnace, where they are mixed with oxygen. The combustion gases from the furnace area then flow to an oxygen sensor, and the heat release is calculated based on the amount of oxygen consumed during the combustion process.

The results of the MCC testing are summarized in Figure 3; there is a clear trend that, as the GO content increases, the total heat release and peak heat release capacity decrease. The one exception to this trend is for PC. PC is known to be sensitive to acids and bases such that the presence of acid or base can have negative effects on flame retardancy

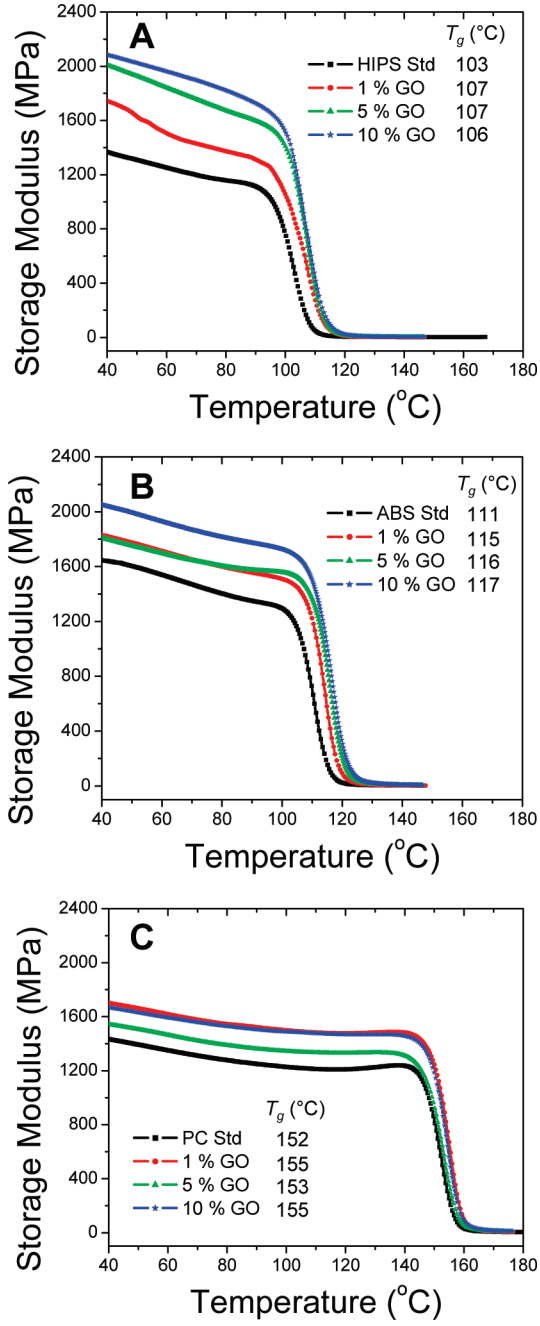

FIGURE 2. DMA storage modulus with increasing temperature for GO composites made with HIPS (A), ABS (B), and PC (C) systems. The T_g values for each sample are shown in the insets. For all systems, the storage modulus increases with the addition of GO over a wide temperature range.

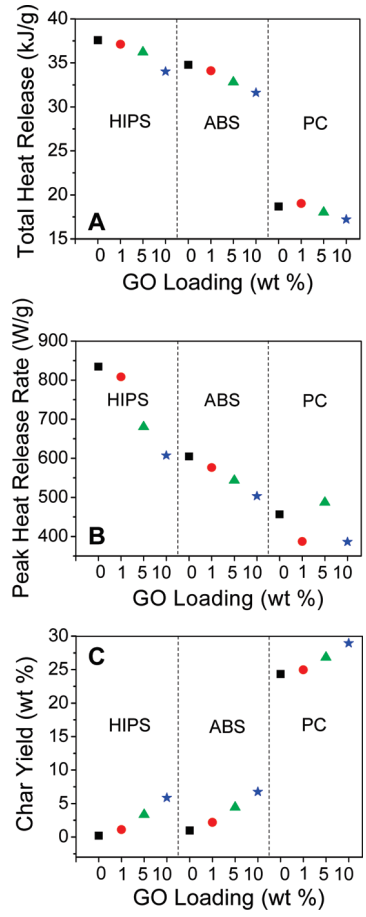

FIGURE 3. MCC results for GO–HIPS, GO–ABS, and GO–PC nanocomposite systems. There is a clear trend that the total heat release (A) and peak heat release rate (B) both decrease as the GO content is increased in all polymers. The char yield (C) also increases for all polymer systems as GO is increased, but this seems to be an additive effect.

(28–30). At low loading (1 wt %), the effects of GO on the heat release are minimal, but at 5 wt %, one sees a negative effect on the flammability in both the peak heat release and the total heat release, likely caused by the acidic groups at high enough concentration to result in PC molecular weight degradation and therefore a higher heat release (less PC polymer structure converts to char). At 10 wt % GO, enough of a network structure has been formed such that the GO can lower the heat release/mass loss and counter the effects of the acidic groups on the GO surface. So, perhaps with the exception of PC, it appears that GO has therefore effectively decreased the flammability of the materials tested. However, while the char yield increases as GO is increased, the collected char yields do not appear to be more than additive effects. In fact, it appears that about half of the GO is consumed during the experiment; otherwise, the char yields would be even higher, assuming that 10 wt % GO is thermally stable up to 900 °C. An additional effect noted is that, at 10 wt % GO loadings, the polymer sample stops melting and flowing before becoming a char. The appearance of small black dots/char "lumps" roughly in the shape of the starting sample was noted in the 10 wt % GO samples, which is a characteristic also seen in carbon nanotubes, carbon nanofibers, and clay nanocomposites with good nanoparticle dispersion and low heat release behavior (31). It is also a feature of a material with antidripping behavior (high melt viscosity) during burning (12, 13). Additionally, the heat release rate curve shape (see Figure S1 in the Supporting Information) is unchanged when the control sample is compared to the GO-containing samples. This indicates that GO is only slowing down the rates of mass loss/fuel pyrolysis and is most likely not changing the thermal decomposition profile/chemistry of the sample. While we do not have TGA–Fourier tranform IR or other evolved gas analysis data to prove this exactly, on the basis of the work by Wilkie, we can roughly make that assessment in light of

Table 1. Selected Results from TGA and Vertical Fire Testing

sample	dec onset (°C)[a]	temp at max wt loss rate (°C)[a]	time to self-extinguish (s)	obsd dripping	time before first drip (s)	sample remaining
HIPS standard	384	423	n/a	yes	12	no
1% GO in HIPS	384	418	n/a	yes	14	no
5% GO in HIPS	399	426	n/a	yes	17	no
10% GO in HIPS	386	421	n/a	yes	24	no
ABS standard	381	424	68	yes	68	yes
1% GO in ABS	374	413	21	yes	68	yes
5% GO in ABS	366	406	33	yes	33	yes
10% GO in ABS	371	411	79	yes	79	yes
PC standard	475	508	14	yes	14	yes
1% GO in PC	471	505	4	no	n/a	yes
5% GO in PC	475	508	0	no	n/a	yes
10% GO in PC	477	507	0	no	n/a	yes

[a] The temperature of decomposition onset is defined as the temperature at which 5 wt % weight loss occurred. The temperature at the maximum weight loss rate is the temperature at the maximum of the derivative curve.

how carbon nanotubes and nanofibers (which have surface chemistry similar to that of GO) affect the polymeric flammability (32). Namely, they produce a network structure that slows down mass loss but does not change the polymer decomposition chemistry/decomposition profile.

TGA was performed to assess the general thermal stability of the GO composites compared to the as-received material. In general, the thermal profile of the GO composites did not change significantly from that of the starting material. Table 1 gives the results of the decomposition onset temperature, defined as the temperature at which 5 wt % weight loss occurred, and the temperature of the maximum weight loss rate (peak of the derivative curve). The TGA thermograms and corresponding derivative curves may be found in Figure S2 in the Supporting Information. For the HIPS systems, the temperatures remained fairly constant, except for the 5 wt % GO sample, which increased both the decomposition onset and the maximum weight loss rate temperatures (from 384 to 399 °C and from 423 to 426 °C, respectively). For the ABS systems, both temperatures decreased slightly with increasing GO addition (from 381 to 371 °C and from 424 to 411 °C for the 10 wt % GO sample), indicating a slight decrease in the thermal stability. Both temperatures for the PC systems remained constant for all GO loadings. Therefore, it can be concluded that the addition of GO does not significantly alter the thermal stability of the polymer resin to which it is added.

To further assess the material flammability, especially the ability of a molten polymer to drip and spread flame in a fire, vertical open flame testing was performed on a plastic sample, molded into the shape of a rectangular bar (1.3 cm wide, 7.6 cm long, and 0.3 cm thick) that is suspended above a cotton patch. The plastic bar is exposed to a 10 s ignition with a methane-fueled flame that is contained in a flame-testing hood free of passing air currents. After the 10 s ignition period, the flame is removed and the time for the polymer to self-extinguish is recorded. Sample dripping and cotton ignition are also noted. The test performed was a modified version of ASTM D3801; on the basis of the actual flame height that was used, the test method can be classified as being between the UL-V0 (ASTM D3801) and UL-94 5 V (ASTM D5048) tests in severity (33). These methods typically give ratings of V-0, V-1, and V-2 to materials based on the self-extinguishing time and dripping behavior; however, because the method used was not an exact match to the UL-94 specifications, such assignments cannot be made. Unlike MCC, this type of testing can provide a general assessment as to how GO affects the material's drip behavior in a flaming drip fire risk scenario, which is important to real-world fire safety applications. The vertical fire test results for all composites are summarized in Table 1. As expected, the GO−PC composites displayed the best results; the self-extinguishing times for 5 and 10 wt % GO in PC were immediate after removal of the flame. Although the self-extinguishing times of the ABS systems were considerably longer, the behavior of the burning material suggests flame-retarding behavior with increasing GO content. The ABS standard (no GO present) began elongating almost immediately after removal of the flame until almost the entire sample dripped after 68 s. With only 1 wt % GO in ABS, the sample did not elongate as drastically. After ~20 s, a small portion of the sample dripped (and ignited the cotton), but most of the sample remained and extinguished immediately after the drip occurred. Similar behavior was observed for 5 and 10 wt % GO in ABS; elongation was diminished such that dripping was only limited to a small portion of the sample and the remaining sample self-extinguished. As expected, the HIPS samples, being the most flammable starting material, performed the worst in the flame tests. The standard dripped several times (the first time only 12 s after the flame was removed) and never self-extinguished. The addition of GO to HIPS only increased the amount of time until the first drip; all samples continued burning, even after portions had dripped, until all of the sample was completely consumed. So, while GO may reduce the mass loss rate, it may not be forming as robust a network structure (and subsequent viscosity increase) responsible for the flammability reduction and antidrip behavior for other polymer nanocomposites (12, 31).

Despite the poor flame test results for ABS and HIPS, it appears that GO is still an effective additive for lowering the flammability of host polymers. In fact, it has been shown that nanocomposites may display good flame-retardant properties while failing flammability tests similar to UL-94 (34). Further, the behavior of the heat release and vertical fire tests do not correlate because they are two very different tests (35). This is important to note because open flame tests alone cannot measure the absolute flammability performance, nor does it suggest that the material will provide a high level of fire safety in all fire risk scenarios. However, the observations of the sample behavior on burning with this open flame test combined with MCC and TGA data demonstrate the ability of GO to act as a flame-retardant additive.

Flame-Retardant Mechanism. The origin of the flame-retarding behavior of GO is thought to be its ability to form a continuous, protective char layer that acts as a thermal insulator and a mass transport barrier (36). This heat-shielding layer slows down the escape of volatile products generated from the degrading polymer. The reductions in the mass loss rate observed by TGA, the increases in the char yield (less polymer is being pyrolyzed), and the increases in the melt viscosity all suggest that, for GO nanocomposites, the mechanism of flame retardancy is likely a condensed-phase phenomenon due to the formation of a thermal protection/mass loss barrier. The key to achieving this sort of behavior with GO, as with all nanocomposites, is having good dispersion of the nanofiller within the host matrix. The solvent blending and mechanical mixing techniques employed to prepare the samples presented here result in well-dispersed GO within PC, ABS, and HIPS, such that the flammability of the composites was significantly decreased with additions of GO as little as 1 wt %. However, to truly elucidate the mechanism of how the GO particles form this barrier will require additional research, including rheology studies, melt viscosity measurements, and SEM/TEM work of samples in different states of thermal decomposition (pre- and postignition samples as well as post-fire samples).

CONCLUSIONS

GO was blended at 1, 5, and 10 wt % into the commodity polymers HIPS, ABS, and PC to serve as a flame-retarding nanoadditive. MCC, TGA, and vertical open flame testing demonstrated the diminished flammability of the material as the amount of GO was increased; the total heat release and peak heat release rate decreased while the char yield increased. In addition, SEM and optical microscopy showed that GO was well-dispersed throughout the composite. DMA revealed that the storage modulus increased as the GO loading is increased, and T_g of the polymer increased slightly. This work reveals that GO shows some promise toward the fabrication of polymer nanocomposites in which decreased flammability is desired.

Acknowledgment. The authors thank Richard Lyon of the Federal Aviation Administration (FAA) for helpful discussion and advice. Funding was provided by the FAA (Grant 2007G010), the AFOSR, and the Advanced Energy Consortium.

Supporting Information Available: Heat release curves and TGA data (Figures S1 and S2). This material is available free of charge via the Internet at http://pubs.acs.org.

REFERENCES AND NOTES

(1) Beyer, G. In *Flame Retardant Polymer Nanocomposites*; Morgan, A. B., Wilkie, C. A., Eds.; John Wiley & Sons, Inc.: Hoboken, NJ, 2007; pp 163−190.
(2) Blomqvist, P.; Rosell, L.; Simonson, M. *Fire Technol.* **2004**, *40*, 39–58.
(3) Blomqvist, P.; Rosell, L.; Simonson, M. *Fire Technol.* **2004**, *40*, 59–73.
(4) Levchik, S. V.; Weil, E. D. *J. Fire Sci.* **2006**, *24*, 345–364.
(5) Vaia, R. A.; Maguire, J. F. *Chem. Mater.* **2007**, *19*, 2736–2751.
(6) Paul, D. R.; Robeson, L. M. *Polymer* **2008**, *49*, 3187–3204.
(7) Winey, K. I.; Vaia, R. A. *MRS Bull.* **2007**, *32*, 314–322.
(8) Bredeau, S.; Peeterbroeck, S.; Bonduel, D.; Alexandre, M.; Dubois, P. *Polym. Int.* **2008**, *57*, 547–553.
(9) Jang, B. Z.; Zhamu, A. *J. Mater. Sci.* **2008**, *43*, 5092–5101.
(10) Modesti, M.; Lorenzetti, A.; Simioni, F.; Camino, G. *Polym. Degrad. Stab.* **2002**, *77*, 195–202.
(11) Shi, L.; Li, Z.-M.; Xie, B.-H.; Wang, J.-H.; Tian, C.-R.; Yang, M.-B. *Polym. Int.* **2006**, *55*, 862–871.
(12) Kashiwagi, T.; Du, F.; Douglas, J. F.; Winey, K. I.; Harris, R. H.; Shields, J. R. *Nat. Mater.* **2005**, *4*, 928–933.
(13) Kashiwagi, T.; Du, F.; Winey, K. I.; Groth, K. M.; Shields, J. R.; Bellayer, S. P.; Kim, H.; Douglas, J. F.*Polymer* **2005**, *46*, 471–481.
(14) Song, P. a.; Xu, L.; Guo, Z.; Zhang, Y.; Fang, Z. *J. Mater. Chem.* **2008**, *18*, 5083–5091.
(15) Wang, J. Q.; Han, Z. D. *Polym. Adv. Technol.* **2006**, *17*, 335–340.
(16) Dasari, A.; Yu, Z. Z.; Mai, Y. W.; Cai, G. P.; Song, H. H. *Polymer* **2009**, *50*, 1577–1587.
(17) Lerf, A.; He, H.; Forster, M.; Klinowski, J. *J. Phys. Chem. B* **1998**, *102*, 4477–4482.
(18) Steurer, P.; Wissert, R.; Thomann, R.; Mülhaupt, R. *Macromol. Rapid Commun.* **2009**, *30*, 316–327.
(19) McAllister, M. J.; Li, J.-L.; Adamson, D. H.; Schniepp, H. C.; Abdala, A. A.; Liu, J.; Herrera-Alonso, M.; Milius, D. L.; Car, R.; Prud'homme, R. K.; Aksay, I. A. *Chem. Mater.* **2007**, *19*, 4396–4404.
(20) Zhang, R.; Hu, Y.; Xu, J.; Fan, W.; Chen, Z. *Polym. Degrad. Stab.* **2004**, *85*, 583–588.
(21) Zhang, R.; Hu, Y.; Xu, J.; Fan, W.; Chen, Z.; Wang, Q. *Macromol. Mater. Eng.* **2004**, *289*, 355–359.
(22) Wang, J. Q.; Han, Z. D. In *Fire and Polymers IV: Materials and Concepts for Hazard Prevention*; Wilkie, C. A., Nelson, G. L., Eds.; American Chemical Society: Washington, DC, 2005; Vol. 922, pp 172−184.
(23) Uhl, F. M.; Wilkie, C. A. *Polym. Degrad. Stab.* **2004**, *84*, 215–226.
(24) Staudenmaier, L. *Ber. Dtsch. Chem. Ges.* **1898**, *31*, 1481–1487.
(25) Lyon, R. E.; Takemori, M. T.; Safronava, N.; Stoliarov, S. I.; Walters, R. N. *Polymer* **2009**, *50*, 2608–2617.
(26) Morgan, A. B.; Galaska, M. *Polym. Adv. Technol.* **2008**, *19*, 530–546.
(27) Lyon, R. E.; Walters, R. N.*J. Anal. Appl. Pyrolysis* **2004**, *71*, 27–46.
(28) Grause, G.; Sugawara, K.; Mizoguchi, T.; Yoshioka, T. *Polym. Degrad. Stab.* **2009**, *94*, 1119–1124.
(29) Levchik, S. V.; Weil, E. D. *Polym. Int.* **2005**, *54*, 981–998.
(30) Levchik, S. V.; Weil, E. D. *J. Fire Sci.* **2006**, *24*, 137–151.
(31) Morgan, A. B. *Polym. Adv. Technol.* **2006**, *17*, 206–217.
(32) Costache, M. C.; Heidecker, M. J.; Manias, E.; Camino, G.; Frache, A.; Beyer, G.; Gupta, R. K.; Wilkie, C. A. *Polymer* **2007**, *48*, 6532–6545.
(33) *UL-94: Standard for Tests for Flammability of Plastic Materials for Parts in Devices and Appliances*, 5th ed.; Underwriters Laboratories, Inc.: Research Triangle Park, NC, 1996.
(34) Bourbigot, S.; Duquesne, S.; Fontaine, G.; Bellayer, S.; Turf, T.; Samyn, F. *Mol. Cryst. Liq. Cryst.* **2008**, *486*, 325–339.
(35) Morgan, A. B.; Bundy, M. *Fire Mater.* **2007**, *31*, 257–283.
(36) Kashiwagi, T. In *Flame Retardant Polymer Nanocomposites*; Morgan, A. B., Wilkie, C. A., Eds.; John Wiley & Sons, Inc.: Hoboken, NJ, 2007; pp 285−324.

AM900419M